

Technical Notes

Yaw Angle Effect on Flow Structure over the Nonslender Diamond Wing

S. Yayla,* C. Canpolat,* B. Sahin,[†] and H. Akilli[‡]
Çukurova University, 01330 Balcali, Turkey

DOI: 10.2514/1.J050380

I. Introduction

DELTA wings have evolved over the years and are primarily used on many fighter aircraft. As these aircraft become more and more maneuverable, delta-wing vortex dynamics and the understanding of the physics of time-dependent unsteady flows have become substantially important [1]. Several variables affect the delta-wing vortex dynamics. As indicated by Yaniktepe [2], some of these variables are angle of attack, leading-edge geometry, wing thickness, sweep angle, Reynolds number, and freestream conditions. Yaniktepe and Rockwell [3] investigated aerodynamics of the delta wing with a sweep angle of $\Lambda = 38.7^\circ$ for the value of Reynolds number based on the chord length C , which was maintained at $Re = 10^4$. They reported that the nonslender delta wings exhibited more distinctive features than the slender delta wings, especially at a higher angle of attack as a result of the earlier onset of vortex breakdown, which are based on the time-averaged velocity and vorticity distributions in the crossflow plane. Canpolat et al. [4] observed the variation of flow structures on the delta-wing surface with a sweep angle of $\Lambda = 40^\circ$ as a function of the angle of attack α and yaw angle θ , using the dye visualization technique. When the delta wing is under the effect of a yaw angle, the symmetrical flow structure deteriorates, and a vortex breakdown occurs earlier on the windward side of the delta wing, as compared with the leeward side. The main vortices in crossflow planes occur in the inner side close to the central axis of the delta wing. Many small-sized vortices are also evident next to the main rotating vortices. Yayla et al. [5] investigated the flow structure close to the surface of the nonslender diamond wing, both qualitatively and quantitatively, using the dye visualization and the stereoscopic particle image velocimetry (PIV) techniques. It was stated that, when the yaw angle is increased, the locations of vortex breakdowns approach the wing apex, but the other one moves toward the trailing edge. Goruney and Rockwell [6] investigated the near-surface flow structure and topology on a delta wing of low sweep angle having sinusoidal leading edges of varying amplitude and wavelength. Gursul et al. [7] reviewed unsteady aerodynamics of nonslender delta wings, covering topics of shear layer instabilities, structure of nonslender vortices, breakdown, maneuvering wings, and fluid/structure interactions. Yaniktepe and Rockwell [8] characterized the instantaneous and the time-averaged flow structure on the nonslender diamond and lambda planforms by using the PIV technique.

Received 6 December 2009; revision received 22 June 2010; accepted for publication 27 June 2010. Copyright © 2010 by the American Institute of Aeronautics and Astronautics, Inc.. All rights reserved. Copies of this Note may be made for personal or internal use, on condition that the copier pay the \$10.00 per-copy fee to the Copyright Clearance Center, Inc., 222 Rosewood Drive, Danvers, MA 01923; include the code 0001-1452/10 and \$10.00 in correspondence with the CCC.

*Research Assistant, Department of Mechanical Engineering, Faculty of Engineering and Architecture.

[†]Professor, Department of Mechanical Engineering, Faculty of Engineering and Architecture.

[‡]Associate Professor, Department of Mechanical Engineering, Faculty of Engineering and Architecture.

Ozgoren et al. [9] investigated the structure of vortex breakdown and the effect in the surface of the wing of the separated flow region in the case of the high angle of attack over the slender delta wing. They declared that the high angle of attack rather affects the onset of vortex breakdown, spiral vortex structure, and separated flow region. Breitsamter [10] presented selected results from extensive experimental investigations on turbulent flowfields and unsteady surface pressures caused by leading-edge vortices, in particular, for vortex breakdown flow.

Another important parameter for the delta wing is the yaw angle. The influence of sideslip on the flow about a sharp-edged biconvex delta wing of a unit aspect ratio was investigated by Verhaagen and Naarding [11] using flow visualization techniques as well as pressure and force balance measurements. It was observed that the yaw angle affects the structure of the leading-edge vortex, vortex breakdown, and formation of nonsteady flow structure substantially, which is generated after vortex breakdown. Sohn et al. [12] presented the development and interaction of vortices over a yawed delta wing with leading-edge extension (LEX) through offsurface flow visualization using microwater droplets and a laser beam sheet. By sideslip, the coiling, the merging, and the diffusion of the wing and LEX vortices increase on the windward side, whereas they are delayed significantly on the leeward side. Also, the migration behavior of vortices on the windward and leeward sides of the wing change considerably.

A review of experimental data for delta wings under both steady and unsteady conditions was presented from a vortex dynamics point of view by Lee and Ho [13]. Conclusions were derived that vortices on the suction surface provide an important contribution to the lift of a delta wing, especially for the wings with large sweep-back angle. Delery [14] stated that, in three-dimensional flows, boundary-layer separation leads to the formation of vortices formed by the roll up of the viscous flow sheet, previously confined in a thin layer attached to the wall, which suddenly springs into the outer nondissipative flow. Comprehensive reviews of experimental and numerical works on vortex breakdown were reported by Leibovich [15,16], Escudier [17], and Visbal [18].

Sahin et al. [19] concluded that substantial retardation, or delay, in the onset of vortex breakdown, and thereby the development of large-scale concentration of vorticity due to the helical mode of vortex breakdown, are attainable when the leading edge of the delta wing is perturbed at a natural frequency of vortex breakdown. They also found that upstream movement of the onset of vortex breakdown is attainable when the period of excitation frequency is sufficiently large. Akilli et al. [20] used the technique of PIV to characterize the alterations and structure of the leading-edge vortex formed from a

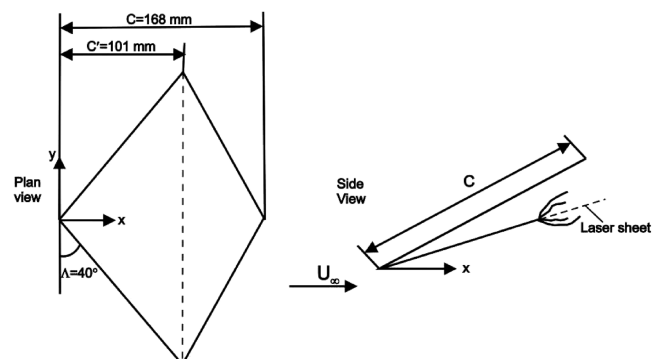


Fig. 1 Schematic of experimental arrangement showing diamond wing and laser-sheet location.

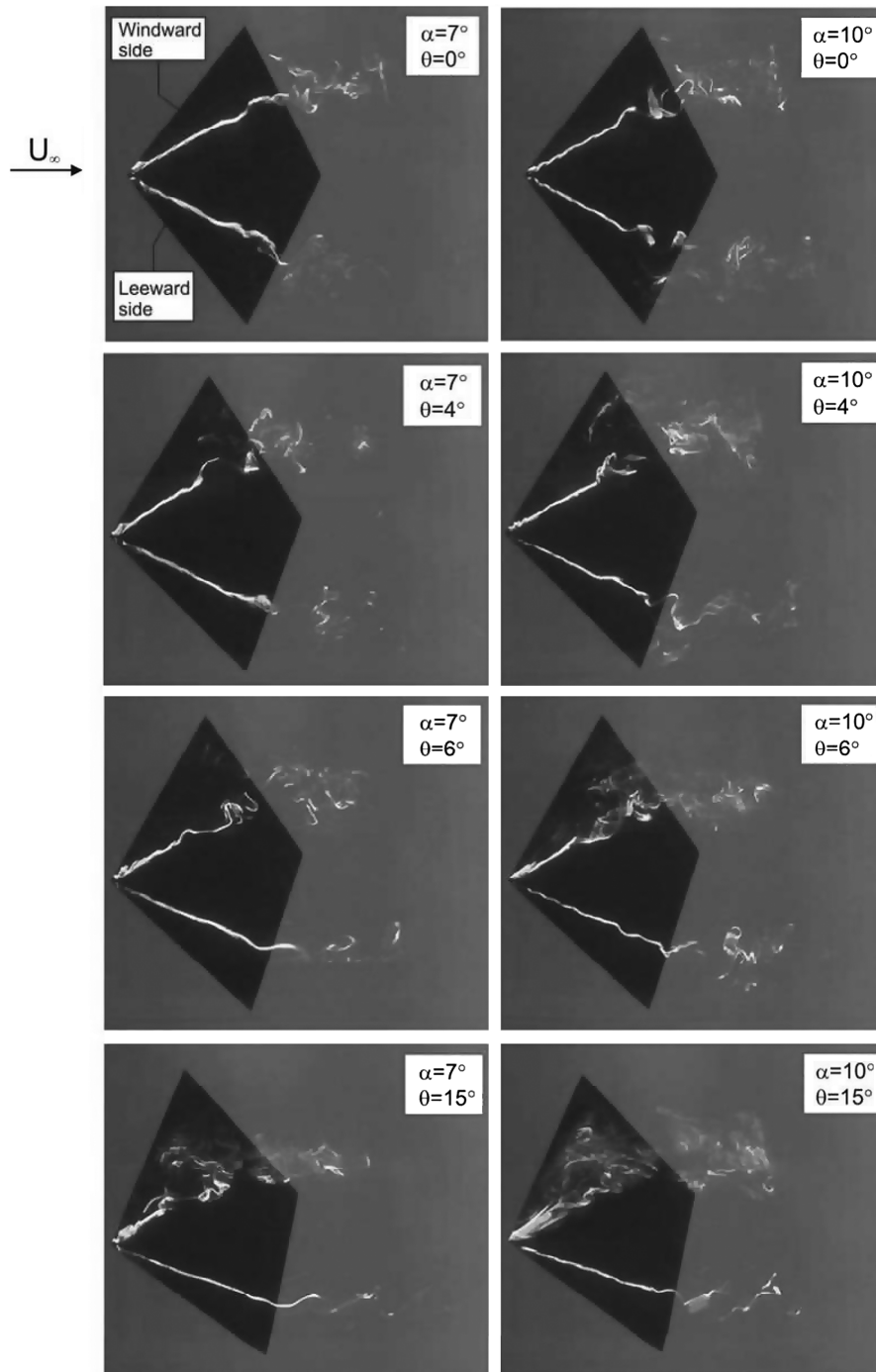


Fig. 2 Formation and development of leading-edge vortex, vortex breakdown, and separated flow region as a function of angle of attack α and yaw angle θ .

delta wing at a high angle of attack in the presence of a small wire oriented orthogonally to the axis of the vortex.

In the present work, the structure of the vortical flow that is characterized within the range of the yaw angle $0^\circ \leq \theta \leq 15^\circ$ for angles of attack of $\alpha = 7$ and 10° is observed on the diamond wing with a $\Lambda = 40^\circ$ sweep angle using dye visualization. There is not much work done on the structure of vortices over nonslender delta wings with sweep angles as low as $\Lambda = 40^\circ$. A review of recent investigations indicates that nonslender wings under angles of attack as low as a few degrees can produce strong vortical flows and the associated unsteady flow phenomena. Yawing the delta wing against freestream flow direction can substantially alter the formation of leading-edge vortices and the onset of vortex breakdown and subsequent unsteady wake flow phenomena. For this reason, present experimental investigation on the unsteady flow over a wide range of

yaw angles provided crucial understanding of the variations of the leading-edge vortex cores, their breakdown behavior, aerodynamic hysteresis, and wing aerodynamic characteristics.

II. Experimental Arrangements and Instrumentations

Dye visualization experiments were conducted in a circulating free-surface water channel. The internal dimensions of the water channel test section, which is made from 15-mm-thick transparent Plexiglas sheet, are $8000 \times 1000 \times 750$ mm. Water flow was driven by a 15 kW centrifugal pump with a speed control unit. Before reaching the test section, flow passes through a two-to-one channel contraction in order to provide a uniform freestream velocity distribution. The depth of the water in the test section was adjusted to a 530 mm height for the present experiments.

Average freestream velocity in the plan-view planes is $U_{av} = 59.5$ mm/s, which corresponds to the Reynolds number $Re_c = 10,000$ based on the chord of the entire diamond wing C and to the Reynolds number $Re_h = 61285$ based on the open-channel hydraulic diameter for all experiments. The chord of the entire diamond wing had a length of 168 mm. Meanwhile, the chord of the leading-edge portion of the diamond wing is $C' = 101$ mm. The sweep angle of the wing was specified as $\Lambda = 40^\circ$. In addition, the wing had a thickness t of 3 mm, and the side edges of the wing were beveled with an angle of 45° . Dimensions of the diamond wing model and the location of the dye visualization plane are shown in Fig. 1. During the dye visualization experiments, the diamond wing model was kept stationary against the freestream flow by a specially designed apparatus that included a servomotor.

The dye visualization technique aims to visualize flow by spreading a certain amount of Rhodamine 6G dye that shines under the laser light exposure in the defined flowfield. The dye visualization technique offers no numerical analysis or data to use, but it shows a brief demonstration of the flow structures. The video camera (Sony HD-SR1) was used to capture the instantaneous video images of the vortex flow structures. Within the scope of this work in the dye experiments, dye was injected in the near field of the delta-wing trailing edge by thin plastic pipe. The needle at the tip of the thin plastic pipe was inserted to a closed and narrow channel embedded in the wing body along the central axis of the delta wing in order to convey the dye directly to the leading edge.

III. Results and Discussion

The results of the dye visualization experiments at angles of attack of $\alpha = 7$ and 10° and yaw angles of $\theta = 0, 4, 6$, and 15° are shown in Fig. 2. In the first column of Fig. 2, the apparent centerlines of leading-edge vortices are clearly identified, and the vortex breakdown occurs after a certain distance from the diamond wing apex close to the trailing edge of the delta-wing attachment for $\alpha = 7^\circ$. The natural flow structure of the diamond wing generally contains a pair of main coherent vortices emanating from the leading edge of the diamond wing and the vortex breakdown, which is defined as the decomposition of the leading-edge vortex occurs.

As seen in the first row of Fig. 2, which presents dye flow visualizations for a zero yaw angle, the location of the vortex breakdown comes closer to the diamond wing apex when the angle of attack is increased from $\alpha = 7^\circ$ to $\alpha = 10^\circ$. Moreover, there is a symmetrical flow structure over the diamond wing in the case of zero yaw angle. When the yaw angle gradually increases, the symmetrical flow structure between both sides of the chord axis of the diamond wing begins to deteriorate. The vortex breakdown location on the leeward side of the diamond wing is delayed when compared to that of the windward side. In other words, the vortex breakdown moves further downstream on the leeward side. As can be seen in Fig. 2 for angles of attack of $\alpha = 7$ and 10° , of the cases of yaw angle less than $\theta = 4^\circ$, the flow structure on both sides of the chord axis of the diamond wing is almost symmetric. Canpolat et al. [4] indicated that the asymmetric flow structure starts at the yaw angle of $\theta = 6^\circ$ for the delta wing having a sweep angle of $\Lambda = 40^\circ$. The leading-edge vortex axis on the windward side of the wing shifts its location toward the central chord axis, and the vortex breakdown occurs at the location further upstream in the case of higher yaw angles θ .

Asymmetrical flow characteristics start at the yaw angle of $\theta = 4^\circ$ in the diamond wing case, when compared with the delta-wing result reported by Canpolat et al. [4]. These changes in the flow characteristics occur due to the trailing-edge configuration attached to the delta wing. At the yaw angle $\theta = 15^\circ$, vortex breakdown occurs in the downstream region of the diamond wing's trailing edge of the leeward side but, on the windward side, the vortex breakdown takes place close to the apex of the wing for both angles of attack $\alpha = 7$ and 10° .

From time to time, a well-defined vortex in the wake flow region downstream of the onset of vortex breakdown reverses back in the anticlockwise direction to form a swirling type of flow that rotates

anticlockwise about its axis, which is perpendicular to the measuring plane (paper plane) and moves in the upstream direction when the yaw angle increases to a value of $\theta = 15^\circ$ at $\alpha = 10^\circ$. In addition, the leading-edge vortex is arced starting from the apex and, later, this curved leading-edge vortex is divided into two branches, as seen in the third images of Fig. 3. Finally, this curved leading-edge vortex turns into an elongated shape and continues to rotate around the straight line as a core vortex; hence, onset of the vortex breakdown moves further downstream, as seen in Fig. 3. Between the curved part of the leading-edge vortex and the windward side edge of the wing, a rather weak swirling-type vortex takes place, rotating about its axis that is perpendicular to the measuring plane. Furthermore, similar observation on the delta wing with sweep angle of $\Lambda = 40^\circ$ was also done by Canpolat et al. [4], as seen in last two images of Fig. 3. In the

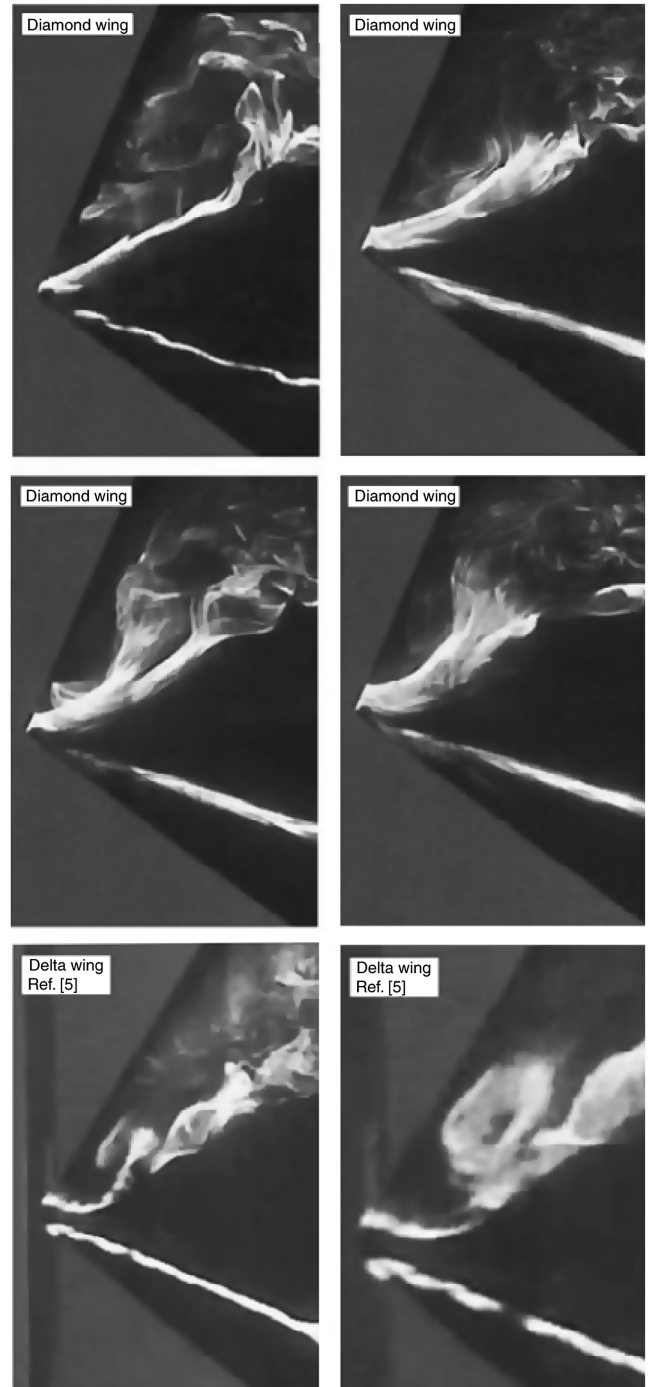


Fig. 3 Formation and distortion of leading-edge vortex, vortex breakdown, and swirling-type vortex for angle of attack, $\alpha = 10^\circ$, and yaw angle, $\theta = 15^\circ$.

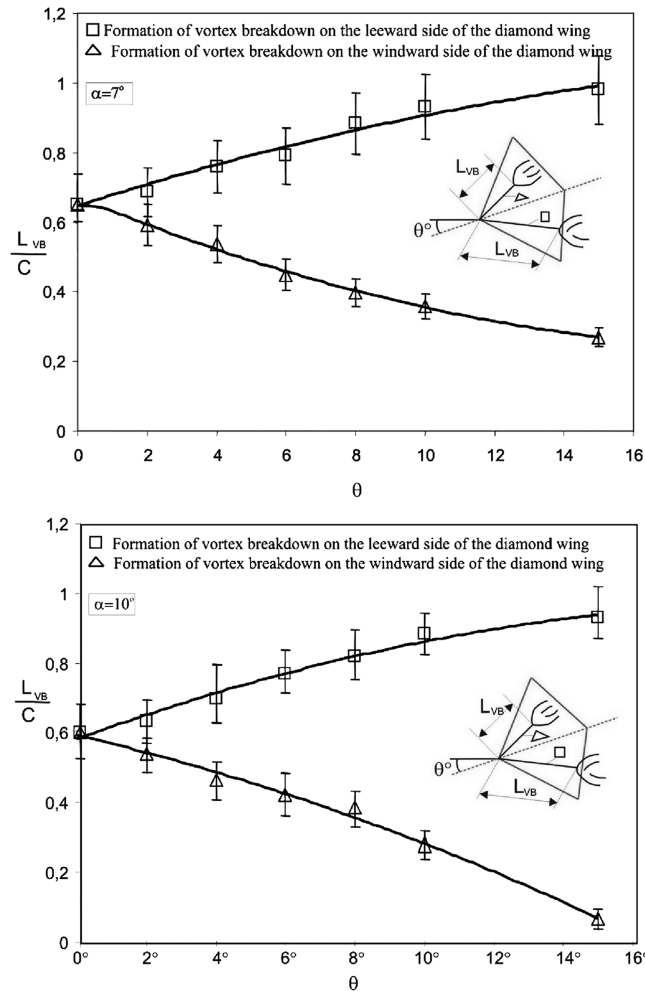


Fig. 4 Location of vortex breakdown L_{VB}/C with yaw angle.

case of the delta wing, this swirling-type (focus) vortex is well defined next to the curved leading-edge vortex when compared to the diamond delta-wing case. In both wing cases, the domain of this swirling-type vortex enlarges its size from time to time on a quasi-periodic basis. When this vortex gets its largest shape, the leading-edge vortex disintegrates in the upper stage, causing the vortex breakdown location to occur close to the apex.

Variation in the dimensionless location of vortex breakdown, L_{VB}/C , against the yaw angle is presented in Fig. 4 for angles of attack of $\alpha = 7$ and 10° . Distance between the leading edge of the wing and the vortex breakdown location is designated as L_{VB} and normalized by chord length as L_{VB}/C . The vortex breakdown location on the windward side moves toward the leading edge of the wing, whereas the vortex breakdown location on the leeward side moves further downstream. For example, the vortex breakdown at a yaw angle of $\theta = 15^\circ$ occurs at a location of $L_{VB}/C = 0.05$ for the angle of attack of $\alpha = 10^\circ$. Video of dye visualization indicates that vortex breakdown developed over the wing is obliged to move backward and forward along the leading-edge vortex axis. These variations are shown with a vertical solid line between two bars on each datum. Finally, it can be concluded that a symmetrical flow structure over the suction surface of the wing deteriorates substantially when the yaw angle is increased to a higher level.

IV. Conclusions

The present investigation focuses on a number of fundamental phenomena, which are the formation and development of leading-edge vortices, the vortex breakdown, and the nonsteady flow structure over a diamond wing. These phenomena are inspected qualitatively using the dye visualization technique. The wing has a

leading-edge sweep angle of $\Lambda = 40^\circ$, and the changes in the flow structure were obtained by varying the yaw angle of the diamond wing within the range of $0^\circ \leq \theta \leq 15^\circ$.

At zero yaw angle, two symmetrical leading-edge vortices emanating from the wing apex are observed. The vortex breakdown and stagnation point occur along the central axis of these vortices. Symmetrical flow structure deteriorates substantially with the yaw angle of the diamond wing. However, this deterioration is not clearly observed for yaw angles less than $\theta = 4^\circ$. When the yaw angle is increased beyond $\theta = 4^\circ$, the vortex breakdown occurs in the downstream region of the diamond wing's trailing edge of the leeward side, but the vortex breakdown takes place further upstream on the windward side.

Acknowledgment

The authors acknowledge the financial support of the Scientific and Technological Research Council of Turkey (TUBITAK) for funding under project number 105M225.

References

- [1] Heron, I., and Myose, R. Y., "On the Impingement of a Von Karman Vortex Street on a Delta Wing," 22nd Applied Aerodynamics Conference and Exhibit, AIAA Paper 2004-4731, Aug. 2004.
- [2] Yaniktepe, B., "Origin and Control of Vortex Breakdown of Unmanned Combat Air Vehicles," Ph.D. Thesis, Univ. of Çukurova, Balcali, Turkey, 2006.
- [3] Yaniktepe, B., and Rockwell, D., "Flow Structure on a Delta Wing of Low Sweep Angle," *AIAA Journal*, Vol. 42, No. 3, March 2004, pp. 513–523. doi:10.2514/1.1207
- [4] Canpolat, C., Yayla, S., Sahin, B., and Akilli, H., "Dye Visualization of the Flow Structure over a Yawed Nonslender Delta Wing," *Journal of Aircraft*, Vol. 46, No. 5, 2009, pp. 1818–1822. doi:10.2514/1.45274
- [5] Yayla, S., Canpolat, C., Sahin, B., and Akilli, H., "Effect of Yaw Angle on the Formation of Vortex Breakdown over the Diamond Wing," *Journal of Thermal Science and Technology*, Vol. 30, No. 1, 2010, pp. 79–89.
- [6] Gorunev, T., and Rockwell, D., "Flow Past a Delta Wing with a Sinusoidal Leading Edge: Near-Surface Topology and Flow Structure," *Experiments in Fluids*, Vol. 47, No. 2, 2009, pp. 321–331. doi:10.1007/s00348-009-0666-x
- [7] Gursul, I., Gordnier, R., and Visbal, M., "Unsteady Aerodynamics of Nonslender Delta Wings," *Progress in Aerospace Sciences*, Vol. 41, No. 7, 2005, pp. 515–557. doi:10.1016/j.paerosci.2005.09.002
- [8] Yaniktepe, B., and Rockwell, D., "Flow Structure on Diamond and Lambda Planforms: Trailing-Edge Region," *AIAA Journal*, Vol. 43, No. 7, 2005, pp. 1490–1500. doi:10.2514/1.7618
- [9] Ozgoren, M., Sahin, B., and Rockwell, D., "Vortex Structure on a Delta Wing at High Angle-of-Attack," *AIAA Journal*, Vol. 40, No. 2, 2002, pp. 285–292. doi:10.2514/2.1644
- [10] Breitsamter, C., "Unsteady Flow Phenomena Associated With Leading-Edge Vortices," *Progress in Aerospace Sciences*, Vol. 44, No. 1, 2008, pp. 48–65. doi:10.1016/j.paerosci.2007.10.002
- [11] Verhaagen, N. G., and Naarding, S. H. J., "Experimental and Numerical Investigation of Vortex Flow over a Sideslipping Delta Wing," *Journal of Aircraft*, Vol. 26, No. 11, 1989, pp. 971–978. doi:10.2514/3.45869
- [12] Sohn, M. H., Yong, L., Lee, K. Y., and Chang, J. W., "Vortex Flow Visualization of a Yawed Delta Wing with Leading-Edge Extension," *Journal of Aircraft*, Vol. 41, No. 2, 2004, pp. 231–237. doi:10.2514/1.9281
- [13] Lee, M., and Ho, C. M., "Lift Force of Delta Wings," *Applied Mechanics Reviews*, Vol. 43, No. 9, 1990, pp. 209–221. doi:10.1115/1.3119169
- [14] Delery, J. M., "Aspects of Vortex Breakdown," *Progress in Aerospace Sciences*, Vol. 30, No. 1, 1994, pp. 1–59. doi:10.1016/0376-0421(94)90002-7
- [15] Leibovich, S., "The Structure of Vortex Breakdown," *Annual Review of Fluid Mechanics*, Vol. 10, No. 1, 1978, pp. 221–246. doi:10.1146/annurev.fl.10.010178.001253

- [16] Leibovich, S., "Vortex Stability and Breakdown: Survey and Extension," *AIAA Journal*, Vol. 22, No. 9, 1984, pp. 1192–1206. doi:10.2514/3.8761
- [17] Escudier, M. P., "Vortex Breakdown: Observations and Explanations," *Progress in Aerospace Sciences*, Vol. 25, No. 2, 1988, pp. 189–229. doi:10.1016/0376-0421(88)90007-3
- [18] Visbal, M. R., "Computational and Physical Aspects of Vortex Breakdown on Delta Wings," *33rd Aerospace Sciences Meeting and Exhibit*, AIAA Paper 1995-0585, 1995.
- [19] Sahin, B., Akilli, H., Lin, C. J., and Rockwell, D., "Vortex Breakdown-Edge Intersection: Consequence of Edge Oscillations," *AIAA Journal*, Vol. 39, No. 5, 2001, pp. 865–876. doi:10.2514/2.1390
- [20] Akilli, H., Sahin, B., and Rockwell, D., "Control of Vortex Breakdown by a Transversely-Oriented Wire," *Physics of Fluids*, Vol. 13, No. 2, 2001, pp. 452–463. doi:10.1063/1.1336809

A. Naguib
Associate Editor